In situ ellipsometric monitoring of complex multilayer designs

Svetlana Dligatch

Commonwealth Scientific and Industrial Research Organisation, Materials Science and Engineering,
PO Box 218, Lindfield, NSW 2070, Australia
E-mail: svetlana.dligatch@csiro.au

Received October 30, 2009

Current developments in optical multilayer design and computation make it possible to calculate filters that satisfy the most demanding optical specifications. Some of the designs are highly sensitive to manufacturing errors and require accurate monitoring and control during thin film deposition. Ellipsometric monitoring enables the accurate deposition of any thickness, including very thin layers, and *in situ* measurement of both refractive index and thickness of the layers during deposition, which facilitate the subsequent real-time design reoptimisation. In this letter, a number of complex multilayer designs with the aid of ellipsometric monitoring are presented, including a laser notch plus band-blocker filter, dichroic filter, beamsplitter, and a wide-range broadband multiplayer antireflection coating.

OCIS codes: 240.2130, 310.1860, 120.2130.
doi: 10.3788/COL201008Sl.0044.

In recent years, significant progress has been made in the field of multilayer optical coating design[1−5]. Nearly any optical filter specification can be designed theoretically, and a number of solutions have become available for very complex and challenging structures. Unfortunately, the required accuracy and reproducibility of the properties of a material for such structures are sometimes so high that mass production may be impossible, even in state-of-the-art deposition systems. Hence, the accuracy of *in situ* monitoring and effective feedback control of the deposition process remain significant issues to be addressed.

A number of well-established optical and non-optical techniques allow the monitoring and control of the layer deposition process[6]. The applicability of a particular method is dependent on the deposition technique and the design requirements. For a deposition process being able to maintain a constant rate and stability of the optical constants of the material, satisfactory results can be achieved by using a simple time-termination process. Deposition for a specific period is often adequate for the sputtering techniques when the required accuracy of film thickness is within a few nanometres[7−9]. However, in many coating methods, including evaporation, the material refractive index, and deposition rate resulting from simply timing the deposition are not sufficiently stable to produce precise optical filter coatings. Quartz crystal monitoring, another frequently used non-optical method for thickness monitoring, indirectly measures the deposition rate and film thickness. It is simple, easy to install, and relatively cheap. However, the random thickness errors of the crystal monitoring systems used in production are in the order of 4%[10], which makes it inadequate for the production of certain complex optical structures. Optical *in situ* monitoring can produce much better results since the monitoring is conducted using the optical parameters of the structure, which are more directly related to the end performance. Optical monitoring techniques can be subdivided into two major categories: photometric methods (e.g., reflection, transmission, and others) and polarisation-dependent methods (e.g., ellipsometry, polarimetry, and others). Many optical designs can be successfully produced using single or multi-wavelength photometric monitoring. Single wavelength optical monitoring is the most widely used production technique. Turning point[11] and level monitoring[12,13] are the popular single wavelength monitoring methods suitable for designs based on periodic quarterwave optical thickness (QWOT).

Broadband transmittance and/or reflectance have been widely used for deposition monitoring of non-quarterwave designs over the last three decades[14]. The enhancement of the computational power of modern computers has boosted the practical application of photometric methods and has led to the increased capability in data processing and deposition control. For example, sub-nanometre accuracy in thickness control has been reported for single layer deposition[15]. Real-time reoptimisation based on broadband reflectance and transmittance data has been implemented for the manufacture of high-performance non-quarterwave designs[16]. Moreover, advances in broadband photometric monitoring have allowed nanometre-level thickness control in multilayer production.

Ellipsometry is one of the most widely used polarisation-dependent methods. *In situ* ellipsometry has been successfully applied to a diverse range of applications in both research and industry. It is relatively simple, reliable, and provides highly accurate real-time measurements of both the thickness and refractive index of growing layers[17−20]. It also provides robust information for the reoptimisation of the design according to the measured properties of the deposited layer. In many cases, this can be accomplished without interrupting of the deposition process. Owing to its advantages, ellipsometry has grown in popularity. It has been extensively used in the study of optical thin film material properties and in the monitoring of multilayers with demanding specifications[21−26].

1671-7694/2010/S10044-05

Ellipsometry is a century-old technique, and its theory and applications are covered at length[17−20]. Progress in the automation of ellipsometric instruments started in the early 1960s and has accelerated significantly during the last decade. The introduction of fast and inexpensive computers has allowed the development of broadband spectroscopic ellipsometers with the latest commercial instruments, enabling their expansion into both the vacuum ultraviolet and mid-infrared ranges[27]. Currently, high-accuracy data can be acquired over broad spectral ranges within seconds[28]. Improvements in ellipsometric instrumentation have advanced research and industrial capabilities in traditional areas such as multilayer optical coatings, and have triggered the development of a new range of applications[19].

Ellipsometry has a number of advantages compared with conventional photometric monitoring. Unlike photometric monitoring, where only one value is obtained per measurement, ellipsometers measure two ellipsometric values, $\varPsi$ and $\varDelta$. As a result, two parameters of a film can be simultaneously determined for each measurement point: refractive index n, and thickness d. In the case of a bare substrate, the optical constants n and extinction coefficient k can be directly derived from $\varPsi$ and $\varDelta$.

The ellipsometric angles, $\varPsi$ and $\varDelta$, are defined (for reflection) in Eq. (1). In this equation, ρ is defined as the complex ratio of the Fresnel reflection coefficients for p-polarised light to that for s-polarised light[17].

$$\begin{aligned}\rho &= \frac{r_\mathrm{p}}{r_\mathrm{s}} = \frac{|r_\mathrm{p}|\exp(\mathrm{i}\delta_\mathrm{p})}{|r_\mathrm{s}|\exp(\mathrm{i}\delta_\mathrm{s})} = \left|\frac{r_\mathrm{p}}{r_\mathrm{s}}\right| \exp\mathrm{i}(\delta_\mathrm{p}-\delta_\mathrm{s}) \\ &= \tan\varPsi \exp\mathrm{i}\varDelta, \qquad (1)\end{aligned}$$

where r_p and r_s are the Fresnel reflection coefficients, $|r_\mathrm{p}|$ and $|r_\mathrm{s}|$ are the amplitude terms, and δ_s and δ_p are the phase change on the reflection terms for p- and s-polarised light, respectively.

Traditionally, ellipsometers are divided into four major groups: early single wavelength nulling and principal angle[29,30], division-of-amplitude[31,32], phase-modulated[33], and rotating element[34]. The merits and limitations of different configurations are discussed in detail[18−20]. All the multilayers presented in this letter were manufactured using a multi-laser line (up to five wavelengths from the visible to near-infrared (NIR) region) rotating analyser ellipsometer (RAE) constructed in-house, as described in detail in the reports of Netterfield *et al.* and Hauge *et al.*[35,36]. The basic setup of the instrument is shown in Fig. 1.

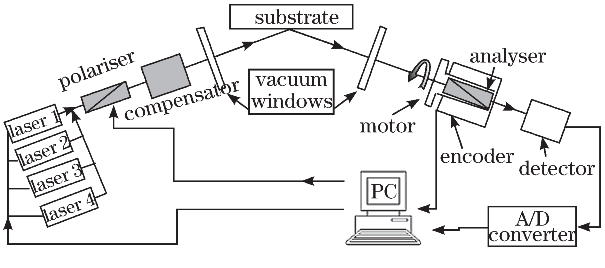

Fig. 1. Setup of the multi-laser line rotating analyser ellipsometer.

An incident laser wavelength is selected by the computer, then polarised on transmittance through a computer-controlled Glan-Thompson polariser that can be set to any angle within 0.02°. To increase the accuracy of the measurement of $\varDelta$[36], a quarterwave plate compensator is used when $\varDelta$ is approximately ±10° of either 0° or 180°. The compensator optical axis is set at approximately 45° to the plane of incidence. Light then passes through the vacuum window at normal incidence and onto the sample. The angle of incidence is ~70° and all angles can be measured up to 0.01° accuracy. The reflected beam exits the vacuum system through another window (which is also orthogonal to the light beam), passes through the analyser, and then onto a silicon detector. The analyser rotates at a constant frequency of up to 10 Hz. The signal intensity is measured using a 16-bit analogue-to-digital (A/D) converter at 225 equally spaced angular positions over a full revolution. The measured intensity of the signal $I(\theta)$ is related to the azimuth of the transmitting axis of the analyser θ by the following equation[36]:

$$I(\theta) = I_0(1 + a\cos 2\theta + b\sin 2\theta), \qquad (2)$$

where I_0 is the average intensity for a full rotation of the analyser. The coefficients a and b are calculated from a Fourier analysis of the intensity variations as a function of the analyser azimuthal angle, and related to $\varPsi$ and $\varDelta$ by

$$\begin{aligned}\tan\varPsi\exp(\mathrm{i}\varDelta) &= \frac{(1+a)}{[b \pm \mathrm{i}(1-a^2-b^2)^{1/2}]} \\ &\quad \times \frac{\tan C + \rho_\mathrm{c}\tan(P-C)}{1-\rho_\mathrm{c}\tan C\tan(P-C)}, \qquad (3)\end{aligned}$$

where P and C are the azimuths of the fast axes of the polariser and compensator, respectively, and ρ_c is the fast-to-slow complex relative to the transmittance of the compensator

$$\rho_\mathrm{c} = T_\mathrm{c}\exp(-\mathrm{i}\varDelta_\mathrm{c}), \qquad (4)$$

where T_c is the ratio of the transmittances of the compensator along its fast and slow axes, and $\varDelta_\mathrm{c}$ is the relative retardation along the axes.

A number of high-precision optical coatings have been successfully produced using the real-time, multi-wavelength ellipsometry. Crystal monitoring has been used to maintain the stable deposition rate, and a spectrophotometer has been used for broadband transmission (reflection) monitoring. In this letter, several types of multilayer optical filters are presented, including broadband anti-reflection coatings, dichroic mirrors, beamsplitters, and colour-corrected laser protection filters.

All the multilayer filters presented here were produced using an ion-assisted deposition system[37−39] built for the purpose. The high-refractive-index oxide layers and magnesium fluoride were deposited by ion-assisted electron beam evaporation. Likewise, $\mathrm{SiO_2}$ layers were deposited by the ion-assisted reactive thermal evaporation of silicon monoxide in the presence of oxygen.

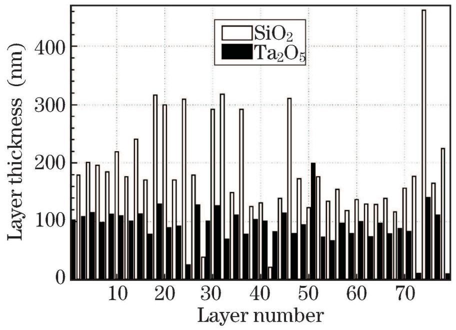

Fig. 2. Optical design of the 79-layer laser protection filter.

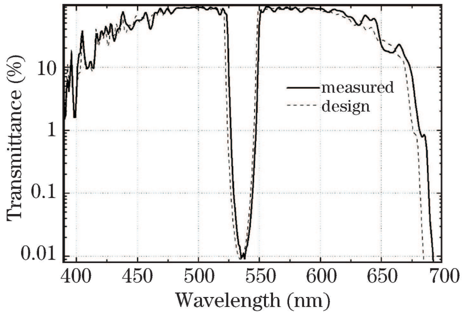

Fig. 3. Measured performance of the laser protection filter.

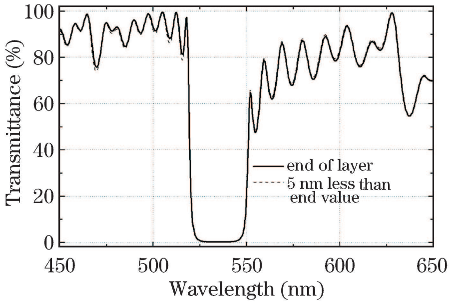

Fig. 4. Plot of the calculated spectral transmittance at the end of layer 48, and at 5 nm less than its termination value.

To date, one of the most difficult optical designs we have fabricated was a colour-corrected, near-infrared blocking with a 532-nm notch laser protection filter[25]. The multilayer optical thin film coating consisted of 79 layers of Ta_2O_5 and SiO_2 of various thicknesses (Fig. 2).

The filter design was extremely sensitive to errors in thickness and deviations of optical properties of the constituent films. Its specifications required an optical density > 4 at 532 nm, optical density > 3 over the 690–1100 nm range, photopic transmittance $> 55\%$ (wherein 60.4% was achieved within 1% of the design value), and colour saturation $< 10\%$ (wherein less than 5% was achieved). The results are shown in Fig. 3.

Laser protection filters require the thickness of each layer to be accurate within 0.5 nm in order to meet the required optical performance specifications. To achieve the high level of control required during the fabrication of such a multilayer optical coating, real-time ellipsometric monitoring is paramount.

The advantage of ellipsometric monitoring over the single or multi-wavelength photometric monitoring was evident in the monitoring of layer 48 in this filter. The calculated spectral transmittance of the multilayer at the end of the layer and the corresponding layer, which was 5 nm less than the correct thickness, is shown in Fig. 4. Note that the figure shows little difference between the curves over the wavelength range 450–650 nm, a typical range for a multi-wavelength transmittance monitoring system.

Considering the uncertainty in the spectrum caused by the errors in the previous layer (i.e., wavelength shift and absolute value), the monitoring substrate run-out due to the rotation, and the drift in the absolute value of the monitoring response, such a method is unlikely to positively resolve the monitoring difference of layer 48, which requires better than a thickness error of approximately 5 nm. Using ellipsometry, there are many wavelength options where the sensitivity at the termination layer is significantly better than a nanometre. For the same layer, Layer 48, the change in Δ over the last 5 nm was 18.7°, and the change for Ψ was 0.28° at the 633-nm monitoring wavelength. Even for an inaccurate ellipsometer, the termination of the layer to $<<$ 1 nm was assured.

Broadband antireflection filters and dichroic coatings present other design challenges. Here, a broadband antireflection coating was designed to achieve a reflectivity of $< 0.5\%$ in the wavelength regions of 400–550 nm and 600–900 nm, and a reflectivity of $< 0.01\%$ at 1319 nm. The calculated and measured optical performance of the broadband anti-reflection coating is shown in Fig. 5. Reflectivity was measured using a Cary-5 spectrophotometer. The reflectivity at 1319 nm was measured separately using a 75-mW laser to verify that the filter satisfied the specified requirement ($< 0.01\%$). The coating was about 1.5-μm thick and consisted of 26 alternating layers of Ta_2O_5 and SiO_2, with MgF_2 as the outside layer[26].

An example of a dichroic filter that requires the sub-nanometre accuracy during fabrication is shown in Fig. 6. This coating was designed to provide high reflectance ($>98\%$) at 650–900 nm and 1319 nm, and high transmittance ($>85\%$) at 400–550 nm. The beamsplitter coating consisted of 24 alternating layers of Ta_2O_5 and SiO_2. The total thickness of the coating was ~ 1.8 μm[26].

Neutral beamsplitter coating is another example of a multilayer design that requires sub-nanometre accuracy in order to meet specifications, as shown in Fig. 7. The beamsplitter coating is sandwiched between two glass flats with an anti-reflection coating on both the outside faces. Here, this component was assembled by optical contacting. The multilayer coating was designed with the following specifications: $0.95 < T_{\rm p,s}/R_{\rm p,s} < 1.05$ in the range of 400–900 nm and 1319 nm ($T_{\rm p,s}$ and $R_{\rm p,s}$ are the transmittance and reflectance for the p- and s-polarisations, respectively). The coating was ~ 3.8-μm thick and consisted of 36 layers of TiO_2 and SiO_2[26].

All the multilayer filters presented here were very sensitive to fabrication errors, in both thickness and refractive index, and required a high level of control of the deposition process. Thus, the given examples indicate that ellipsometric monitoring is a very versatile method and yields good results in a wide range of applications.

In order to achieve a high level of deposition control, the monitoring strategy must be adjusted for each particular design. To monitor the deposition, pre-calculated ellipsometric curves were used for each layer. During the modelling process, it was vital to select the optimum

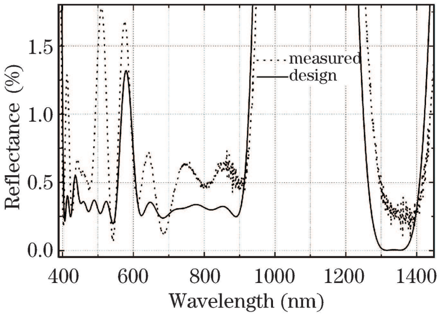

Fig. 5. Designed and measured optical performance of the broadband, anti-reflection coating.

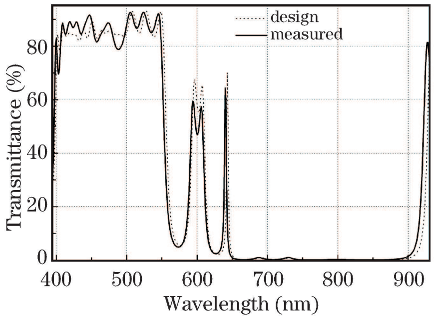

Fig. 6. Measured and calculated transmittance of the dichroic coating.

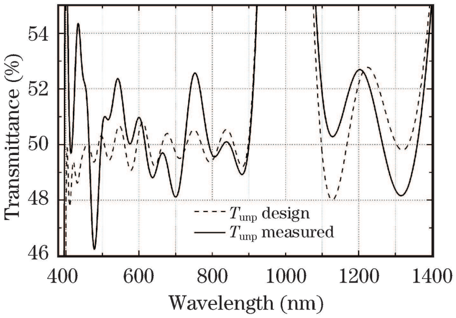

Fig. 7. Designed and measured optical performance of the broadband, neutral sandwiched beamsplitter.

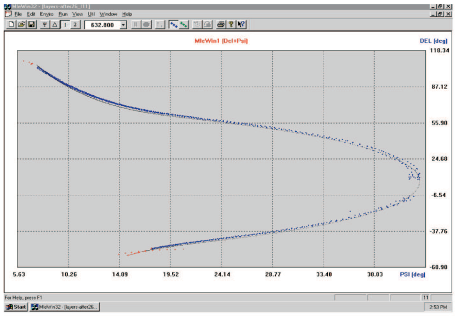

Fig. 8. Pre-calculated curve (solid line) and *in situ* ellipsometric measurements for layer 37 of the laser protection filter described in the previous section.

laser wavelength to achieve sufficient gradients in Δ and Ψ at the end of each layer. These monitoring curves were used to automatically terminate the deposition when the ellipsometric parameters have reached the target values (Fig. 8).

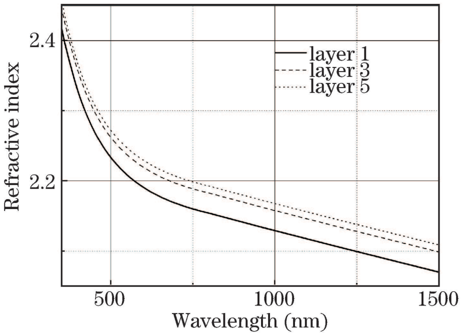

Fig. 9. Typical variation of the refractive index of Ta_2O_5 in layers 1, 3, and 5.

All minor variations of the refractive index during deposition and/or deviations from the targeted layer thickness were computed using the in-house-developed ellipsometric analysis software, and simultaneously taken into account. In our deposition system, the largest refractive index variations were observed in the high refractive index materials at the beginning of a deposition run (Fig. 9). This behaviour is thought to be due to the change in the substrate temperature.

The observed variations in the refractive index and/or thickness of the layers were used in the reoptimisation of subsequent layers.

There are a number of instrumental challenges to overcome in order to obtain precise and accurate ellipsometric measurements in real-time and in a production environment, especially for multilayer coatings. One of the problems is the monitored beam wobble caused by the rotation of the substrate. In most deposition systems, substrate rotation is essential to achieve the required uniformity of the growing film. The rotation of the substrate creates a challenge in alignment, and in maintaining the orthogonality of the rotating substrate to the ellipsometer's plane of incidence with high accuracy (preferably within $< 0.01°$). A number of strategies have been reported to minimise the effect of substrate wobble and improve the signal-to-noise ratio of the ellipsometric measurements[40]. In our system, alignment and calibration procedures were carried out on a rotating substrate (~1 Hz). Time averaging of the measurements was performed to reduce the periodicity induced in the ellipsometric data by the substrate wobble. Computer simulation with all the available wavelengths can be used to determine the best monitoring wavelength for each layer in order to achieve the highest possible sensitivity and lowest error.

Interpretation of *in situ* ellipsometric data requires fitting real-time measurements to a model. To create such a growth model, knowledge regarding the optical properties of the growing film is necessary. Extensive *ex situ* measurements of the optical properties of the deposition materials were carried out and a library of optical constants for the materials was created. In order to reduce the "operator" effect and maintain the optical properties close to those of the design model, a computerised feedback system was developed to control the deposition process.

In order to minimise the coating deviation from the design, special attention was given to the layers with the highest relative sensitivity to errors in the layer thickness during deposition. As a result, deposition processes capable of producing a whole array of broadband optical coatings to sub-nanometre accuracy were developed.

In conclusion, we have demonstrated that *in situ* ellipsometry can be utilised under real-time production conditions to manufacture a range of multilayer structures with high accuracy. Furthermore, future works aimed at extending the capabilities of the *in situ* ellipsometric system to monitor mixed and graded materials whose optical properties are extremely dependent on the deposition conditions are in the planning stages. This improved ellipsometric system would allow small deviations from the targeted parameters to be detected immediately, and conditions to be adjusted to achieve the required optical properties.

Additional improvements in the ellipsometric data processing would include the simultaneous measurement at several wavelengths and the development of more “intelligent” software that will enable more efficient assessment of the sensitivity and error limits for each wavelength.

The author gratefully acknowledges the valuable assistance and vital inputs of Dr. M. Gross, Dr. A. Bendavid, and Dr. A. Chtanov.

References

1. H. A. Macleod, The Essential Macleod, Thin Film Center Inc.
2. TFCalc by Software Spectra, Inc., 14025 N. W. Harvest Lane, Portland, OR 97229 USA.
3. A. V. Tikhonravov and M. K. Trubetskov, *OptiLayer Thin Film*, OptiLayer Consulting Ltd., software copyright, 1997-2003
4. B. T. Sullivan and J. A. Dobrovolski, Appl. Opt. **35,** 5484 (1996).
5. A. V. Tikhonravov, M. K. Trubetskov, and G. W. DeBell, Appl. Opt. **35,** 5493 (1996).
6. H. A. Macleod, Appl. Opt. **28,** 2886 (1989).
7. H. A. Macleod, *Thin film optical filters* (Institute of Physics Publishing, Bristol, 2001).
8. B. T. Sullivan, G. A. Clarke, T. Akiyama, N. Osborne, M. Ranger, J. A. Dobrowolski, and L. Howe, Appl. Opt. **39,** 157 (2000).
9. M. Kobayashi and H. Terui, Appl. Opt. **22,** 3121 (1983).
10. R. R. Willey, *Practical design and Production of thin Films.* (Marcel Dekker, Inc. New York, 2002).
11. D. R. Gibson, P. H. Lissberg, I. Salter, and D. G. Sparks, Opt. Acta **29,** 221 (1982).
12. H. A. Macleod and E. Pelletier, Opt. Acta **24,** 907 (1977).
13. F. Zhao, Appl. Opt. **24,** 33339 (1985).
14. B. Vidal, A. Fornier, and E. Pellitier, Appl. Opt. **18,** 3851 (1979).
15. R. Rabady, K. Zinoviev, and I. Arutsky, Appl. Opt. **43,** 143 (2004).
16. B. Badoil, F. Lemarchand, M. Cathelinaud, and M. Lequime, Appl. Opt. **46,** 4294 (2007).
17. R. M. A. Azzam and N. M. Bashara, *Ellipsometry and Polarised Light* (North Holland, Amsterdam, 1977).
18. E. Wolf, *Progress in Optics* (Elsevier, Amsterdam, 2000).
19. H. G. Tompkins and E. A. Irene, *Handbook of Ellipsometry* (NY & Springer, Heidelberg, 2005).
20. H. Fujiwara, *Spectroscopic Ellipsometry: Principles and Applications* (John Wiley & Sons Ltd., chichester, 2007).
21. B. D. Johs, J. Hale, C. M. Herzinger, T. E. Tiwald, and J. A. Woollam, Proc. SPIE **4449,** 41 (2001).
22. D. E. Morton, B. Johs, and J. Hale, in *Proceedings of SVC 45th Annual Tech.* 299 (2002).
23. J. N. Hilfiker, J. S. Hale, B. D. Johs, T. E. Tiwald, R. A. Synowicki, C. L. Bungay, and J. A. Woollam, in *Proceedings of SVC 44th Annual Tech.* 295 (2001).
24. C. Bungay, J. Hilfiker, M. Liphardt, and R. Synowicki, *Vacuum and Thin Film* 1999.
25. S. Dligatch, R. P. Netterfield, and B. J. Martin, Thin Solid Films **455,** 376 (2004).
26. S. Dligatch, R. P. Netterfield, D. J. Drage, and P. S. Fairman, in *Proceedings of Optical Interference Coatings Conference of the Optical Society of America* (2001).
27. J. N. Hilfiker, C. L. Bungay, R. A. Synowicki, T. E. Tiwald, C. M. Herzinger, B. Johs, G. K. Pribil, and J. A. Woollam, J. Vac. Sci. Technol. A **21,** 1103 (2003).
28. R. W. Collins, J. Koh, H. Fujiwara, P. I. Rovira, A. S. Ferlauto, J. A. Zapien, C. R. Wronski, and R. Messier, Appl. Surf. Sci., **154-155,** 217 (2000).
29. H. Tompkins, *A User’s Guide to Ellipsometry* (Academic Press, San Diego, 1993).
30. M. Yamamoto and O. S. Heavens, Surf. Sci. **96,** 202 (1980).
31. R. M. A. Azzam, Proc. SPIE **2873,** 1 (1996).
32. E. Masetti, M. Motecchi, R. Larciprete, and S. Cozzi, Appl. Opt. **35,** 5626 (1996).
33. S. N. Jasperson and S. E. Schnatterly, Rev. Sci. Instrum. **40,** 761 (1969).
34. B. D. Johs, J. Hale, N. J. Ianno, C. M. Herzinger, T. E. Tiwald, and J. A. Woollam, Proc. SPIE **4449,** 41 (2001).
35. R. P. Netterfield, P. J. Martin, W. G. Sainty, R. M. Duffy, and C. G. Pacey, Rev. Sci. Instrum. **56,** 1995 (1985).
36. P. S. Hauge and F. H. Dill, IBM J. Res. Develop. **17,** 472 (1973).
37. P. J. Martin, H. A. Macleod, R. P. Netterfield, C. G. Pacey, and E. G. Sainty, Appl. Opt. **22,** 178 (1983).
38. R. P. Netterfield, P. J. Martin, C. G. Pacey, W. G. Sainty, D. R. McKenzie, and G. Auchterlonie, J. Appl. Phys. **66,** 1805 (1989).
39. R. P. Netterfield, P. J. Martin, and W. G. Sainty, Appl. Opt. **25,** 3808 (1986).
40. B. Johs, C. Herzinger, J. H. Dinan, A. Cornfeld, J. D. Benson, D. Doctor, G. Olson, I. Ferguson, M. Pelczynski, P. Chow, C. H. Kuo, and S. Johnson, Thin Solid Films **313,** 490 (1998).